JMEPEG (2021) 30:4445–4457
https://doi.org/10.1007/s11665-021-05713-4

1059-9495/$19.00

Investigation on Different TiCn Duplex Treatments Applied to Cold Work Tool Steel for Surface Properties Improvement

Luciano Kempski, Vinicius Waechter Dias, Giovanni Rocha dos Santos, Ricardo Diego Torres, Roberto Hubler, and Alexandre da Silva Rocha

Submitted: 27 October 2020 / Revised: 29 January 2021 / Accepted: 16 March 2021 / Published online: 12 April 2021

In this work, different plasma nitriding and coating thickness combinations were tested to improve surface proprieties of a cold work tool steel. A DIN X100CrMoV8-1-1 cold work tool steel was plasma nitrided, using a 5 vol-%. N2 + 95 vol-% H2 gas mixture, for 2.5- and 5.0-h nitriding times. Then, the non-nitrided and nitrided substrates were coated with titanium carbonitride (TiCN)-graded thin films produced by cathodic arc plasma-assisted physical vapor deposition. Different deposition parameters were used to produce coatings with thicknesses of 1.0 and 2.0 μm. The samples were characterized regarding the microstructure, surface hardness, coating adhesion, and friction coefficient, which were measured by ball-on-disc tests. In the plasma nitriding process, it was possible to generate a diffusion layer, without the formation of a compound layer, with depths of 58 μm and 68 μm for 2.5 and 5.0 h, respectively. Both plasma nitriding treatments avoided delamination of the TiCN coating when deposited on the cold work tool steel. The TiCN coatings significantly decreased the friction coefficient, regardless of substrate condition. The lowest friction values were found for the thinner coating. The deeper diffusion zone led to higher hardness value, and highest scratch crack propagation resistance of the coatings, meaning superior coating adhesion. The best surface properties were found when combining the deeper plasma nitriding diffusion layer with the thinner PVD coating.

Keywords coatings, cold work tool steel, duplex, plasma nitriding, TiCN

1. Introduction

The duplex treatment reduces the hardness difference between a protective coating and the underlying material. The duplex treatment consists of nitriding a steel substrate followed by thin-film deposition, to increase the load-bearing capacity of the coated system. Besides, plasma nitriding can increase the fatigue resistance, strength at elevated temperatures (Ref 1), and wear resistance (Ref 2), especially at high loads (Ref 3). The competitive advantages of duplex treatments and their resulting tribological properties have been reported (Ref 4-8). However, there is still a lack of knowledge regarding the optimum nitriding conditions (e.g., diffusion layer depth) for the most suitable thin-film thickness for the various applications.

A previous work (Ref 9) showed that TiCN PVD arc evaporation coating was a suitable choice to improve performance of cold work tools manufactured from a DIN X100CrMoV8-1-1 steel. The present work presents a more in-depth investigation on the duplex treatment of this steel by changing plasma nitriding parameters to be used before coating, as well as varying TiCN coating parameters to test combinations of different layer thicknesses.

Several studies concluded that the main requirements for achieving suitable quality duplex surface treatments by PVD and nitriding include low roughness of the resulting surface (Ref 10), high compressive residual stresses (Ref 11, 12), and a sufficiently deep nitrided layer to achieve adequate load-bearing capacity (Ref 13). Some results indicate that the presence of a monophasic white layer ε (Ref 14, 15) or γ' (Ref 16, 17) improves coating performance. However, for some grades of tool steel with high carbon content, ε white layer formation is associated with precipitation of carbides and carbonitrides at grain boundaries in the diffusion zone, generating a very brittle microstructure. Besides, ε white layer develops high tensile residual stresses. This combination of properties does not recommend using a white layer for high carbon content tool steels, especially considering forming and cutting tools with edges and corners (Ref 18-20). Therefore, in this investigation, white layer formation has been avoided when using plasma nitriding as a pre-treatment for PVD coating.

This work investigated the duplex treatment of a DIN X100CrMoV8-1-1 cold work tool steel. On the one hand, plasma nitriding was developed to produce steel samples with two different diffusion zone depths without white layer, and on the other hand, TiCN deposition parameters were varied to generate two different coating thicknesses. Non-nitrided and nitrided samples were coated by the different coatings. In order to identify the most promising combinations, the duplex treated samples were characterized regarding chemical composition,

Luciano Kempski, Vinicius Waechter Dias, Giovanni Rocha dos Santos, and **Alexandre da Silva Rocha**, Universidade Federal do Rio Grande do Sul, Porto Alegre, RS, Brazil; **Ricardo Diego Torres**, Pontifícia Universidade Católica do Paraná, Curitiba, Brazil; and **Roberto Hubler**, Pontificia Universidade Catolica do Rio Grande do Sul, Porto Alegre, RS, Brazil. Contact e-mail: viniciuswdias@gmail.com.

microstructure, hardness, coating adhesion, and friction in ball-on-disc tests.

2. Materials and Methods

2.1 Materials and Sample Preparation

Disc specimens with 31 of diameter and 5 mm of thickness were manufactured from a DIN X100CrMoV8-1-1 hot-rolled bar. The steel chemical composition is given by 1.00 wt.% of C; 0.95 wt.% of Si; 7.90 wt.% of Cr; 0.96 wt.% of Mo; and 1.55 wt.% of V. After machining, the samples were heat treated employing a controlled atmosphere heat-treating oven. Samples were tripled tempered at 500 ºC to achieve a final hardness between 60 and 62 HRC. Figure 1 shows the resulting microstructure of a DIN X100CrMoV8-1-1 cold work tool steel specimen after hardening and tempering with primary and secondary carbides.

Before surface treatment, the samples surfaces were ground (#120 to #1200 mesh) and then polished with 1-µm diamond paste to obtain a low final mean roughness (Ra) of 0.023 ± 0.003 μm. Nitriding was carried out in a plasma nitriding furnace equipped with a DC power supply developed in the Department of Metallurgy of the Federal University of Rio Grande do Sul. Plasma nitriding was carried out using five processing steps presented in Table 1. In order to prevent white layer formation during the nitriding step, a gas mixture consisting of 5 vol.% N_2 and 95 vol.% H_2 was used (Ref 9). Two different batches of samples were prepared with nitriding times of 2.5 h (150 min) and 5 h (300 min) to produce two different diffusion layer depths.

After plasma nitriding, the specimens were prepared for subsequent coating deposition by polishing the surfaces with a 1-μm diamond paste to obtain a Ra value of 0.025 ± 0.008 μm and then carefully cleaned and dried. The plasma-assisted cathodic arc evaporation method was used to coat the samples with the TiCN system (Ref 9). Table 2 shows the main process parameters used to deposit coatings with two different thicknesses of 1 and 2 μm. The notations TiCN1 and TiCN2 identify these coatings for the thickness of 1 and 2 μm, respectively. The coated surfaces were post-treated by grinding with #1000 SiC sandpaper to reduce excessive roughness due to surface droplets produced during coating process; such defects are quite common in the cathodic arc deposition method. Table 3 summarizes the processes used to produce each sample group, including the nitriding and coating times and temperatures.

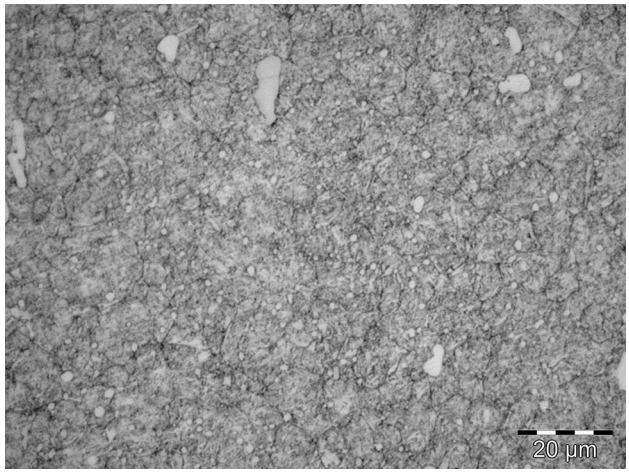

Fig. 1 Optical microscopy cross-sectional view of the DIN X100CrMoV8-1-1 steel used as substrate material in this study

3. Surface Characterization

A standard metallographic preparation method was carried out before the optical microscopy analysis of the nitrided layers. The samples were carefully cut using a precision cutting machine and adequately mounted to promote edge retention to allow observation of the nitrided layers. After mounting, the samples were ground and polished with a 1-µm diamond paste and then etched with a Nital solution (2 vol.% HNO_3 in ethyl alcohol) for optical microscopy analysis. Glow discharge optical spectroscopy (GDOES) determined the carbon and nitrogen content depth profiles.

The coated samples were fractured to provide a cross section of the thin film for scanning electron microscopy (SEM) analysis. x-ray diffraction phase analysis was carried out using a Philips X'Pert MPD diffractometer equipped with Cu-Kα radiation. The interval for data acquisition in 2θ angle was from 30° to 130° with a step size of 0.05° and 15 s/step.

To evaluate hardness and elastic modulus of the coated systems, a Fischerscope HV100 Nanohardness tester equipped with a Berkovich diamond indenter was employed. The measurements were carried out according to the ISO 14577-1:2002(E) standard to measure the Martens hardness and elastic modulus. Hardness and elastic modulus were determined by indenting the surface of the specimens with three loads: (25, 50, or 100 mN), with loading and unloading times of 40 s each. The coated surfaces were indented 10 times for each sample, and each load condition at different locations on the surface. The presented data are the mean value and standard deviations of these measurements.

Adhesion tests were carried out for all coated samples using a Rockwell C indenter according to the DIN 4856 standard (Ref 21). The observed cracks pattern and delamination around the indentations were compared to reference patterns classified in this standard from HF1 to HF4 (good adhesion) and HF5 and HF6 (poor adhesion).

Scratch tests were carried out according to the ASTM C1624-05 (2010) standard using a diamond Rockwell indenter with a tip radius of 200 µm. Normal loads applied to the surface ranged from 1 to 150 N with a loading rate of 5 N/s, indenter displacement velocity of 6 mm/min, and total scratch length of 3 mm. Each sample was scratched three times. The critical load Lc1 was used to identify the first level of cohesive failure, while Lc2 was used to identify the first adhesive failure mode.

The ball-on-disc tribological tests were carried out according to ASTM G99-05 (2010) standard to evaluate the friction coefficient of the TiCN-coated surfaces against aluminum oxide balls in dry conditions. The applied load was 10 N, and the linear velocity of the sphere against the disc (sample) was 0.225 m/s for a total sliding distance of 1000 m. The sphere had a diameter of 6 mm. The calculated hertz maximum contact stress for these conditions was 1.97 GPa (Ref 22). Three tests were done for each sample in different radial positions of the discs (7, 9, and 11 mm).

Table 1 Plasma nitriding parameters for the different treatment steps

	1. Pumping	2. Sputtering	3. Heating and cleaning	4. Nitriding	5. Cooling
Pressure, mbar	Down to 0.05	1	4	4	0.05
Gas mixture, vol.%	…	Pure H_2	Pure Ar	5% N_2/95% H_2	5% N_2/95% H_2
Temperature, °C	…	~ 200	450	450	25
Time, min	Until 0.05 mbar reached	45	Until 450°C reached	150 (2.5 h) or 300 (5 h)	180

Table 2 Coating parameters used to obtain the TiCN1 and TiCn2 samples

	1. Pumping	2. Heating	3. Cleaning	4. Coating	5. Cooling
Pressure (mbar)	Down to 0.005	0.5	0.5	0.02–0.03	300
Gas	–	–	Ar + H_2	C_2H_2 + N_2 + Ar	N_2
Temperatures (°C)					
TiCN1	–	350	350	400	To 25
TiCN2		450	450	450	To 25
Times (min)					
TiCN1	Until 0.005 mbar reached	60	160	38	120
TiCN2		60	160	54	120
Bias	–	–	–	− 200 V	–

Table 3 Identification of the samples according to the process variations

	Applied process	
Samples	**Nitriding time (min)/Nitriding temperature, °C**	**Coating time (min)/Coating temperature, °C**
Non-nitrided	Not coated	Not coated
Nit 2.5	150/450	Not coated
Nit 5	300/450	Not coated
TiCN1	None	38/400
TiCN2	None	54/450
Nit 2.5 + TiCN1	150/450	38/400
Nit 5 + TiCN1	300/450	38/400
Nit 2.5 + TiCN2	150/450	54/450
Nit 5 + TiCN2	300/450	54/450

4. Results and Discussion

4.1 Properties of Plasma-Nitrided Layers

A cross-sectional view of a sample nitrided for 5 h is shown in Fig. 2. Only a nitriding diffusion layer (dark layer) was observed, as expected, for the selected plasma nitriding parameters (temperature of 450°C and gas mixture with 5 vol.% N2). As already known from a previous work (Ref 9), the formation of white layer and grain boundary precipitates in the diffusion layer lead to layer embrittlement, which can be avoided by the selected parameters.

Figures 3 and 4 shows the glow discharge optical spectroscopy (GDOES) carbon and nitrogen concentration profiles. The plasma nitriding layer depth was defined as the distance from the surface at which the nitrogen content reached a minimum of 0.5 at.%. The plasma nitriding diffusion zones of 35 and 45 µm were measured for the nitriding times of 2.5 h and 5 h, respectively. A reduction in the carbon content near the surface compared to the original carbon content of the steel was observed after plasma nitriding, as expected for a plasma-

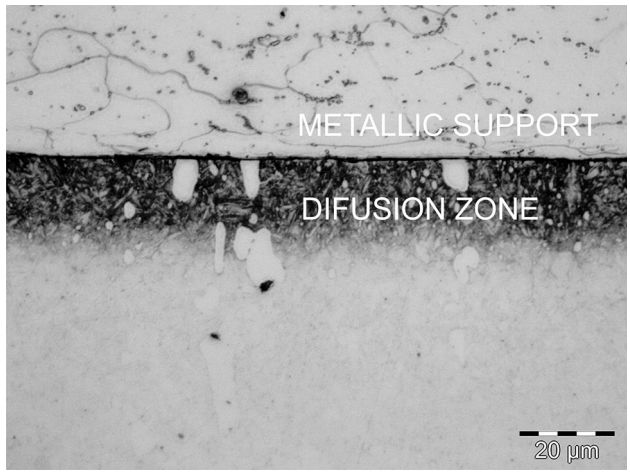

Fig. 2 Optical microscopy cross-sectional view of a sample plasma-nitrided during 5 h

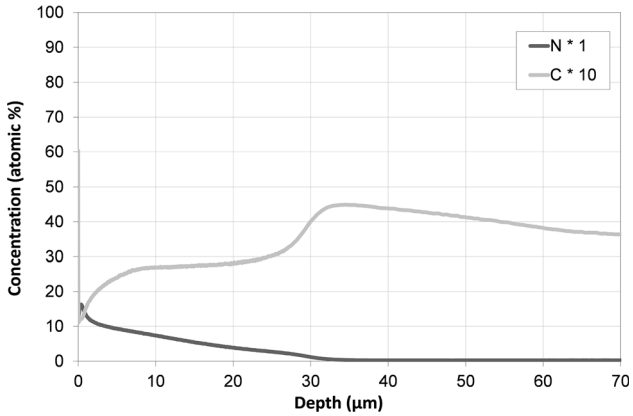

Fig. 3 GDOES chemical composition profile for a sample nitrided during 2.5 h (Nit 2.5)

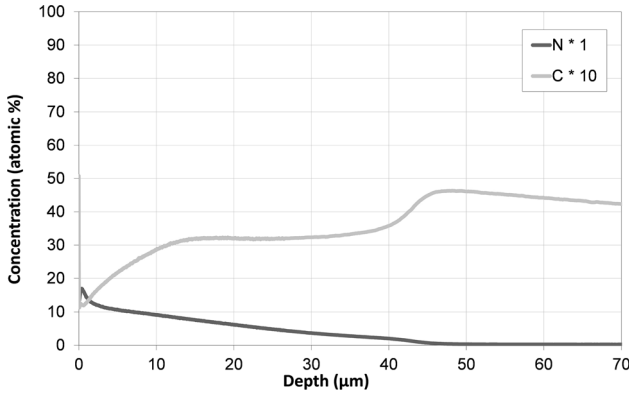

Fig. 4 GDOES chemical composition profile for a sample nitrided during 5 h (Nit 5)

nitrided material without white layer formation. The carbon content below the nitriding diffusion zone increased to a maximum at the depth where the minimum nitrogen concentration was observed, followed by a decrease in the carbon content to the steel substrate's nominal concentration. Such a carbon concentration profile has been observed previously for plasma nitrided samples without compound layers (Ref 19), confirming that no continuous white layer was formed in the samples. The results of the surface microhardness tests with different applied loads are presented in Fig. 5 for the two plasma nitriding times (2.5 h and 5 h); the hardness values were higher for the samples nitrided during 5 h for all applied loads. The difference in the hardness values between the two samples reduces with decreasing load. The highest hardness values of 1550 HV and 1430 HV for 5-h and 2.5-h nitriding time were measured with the lowest test load (0.49 N).

Figure 6 shows the microhardness profiles of the nitrided samples, where the dashed horizontal line indicates the core hardness of the substrate. The nitriding layer depth is determined by the distance from the surface where the hardness reaches the untreated substrate. The nitriding time of 5 h resulted in a higher hardness than the 2.5-h sample over the nitriding layer, as shown previously in Fig. 5. The layer depth for a treatment time of 2.5 h was 58 μm and for 5 h was 68 μm. The substrate average hardness of 750 HV can be converted to around 62 HRC, which shows that the substrate hardness was not affected by the nitriding treatments temperature.

4.2 Properties of Samples after PVD Coating

Figure 7 shows SEM images of the coated samples cross section: (7a) TiCN1 and (7b) TiCN2 coatings. The SEM images revealed that the TiCN coating thickness is around 1.0 µm and 2.0 µm, Also, the images show that both coatings presented a very fine columnar microstructure without visible porosity.

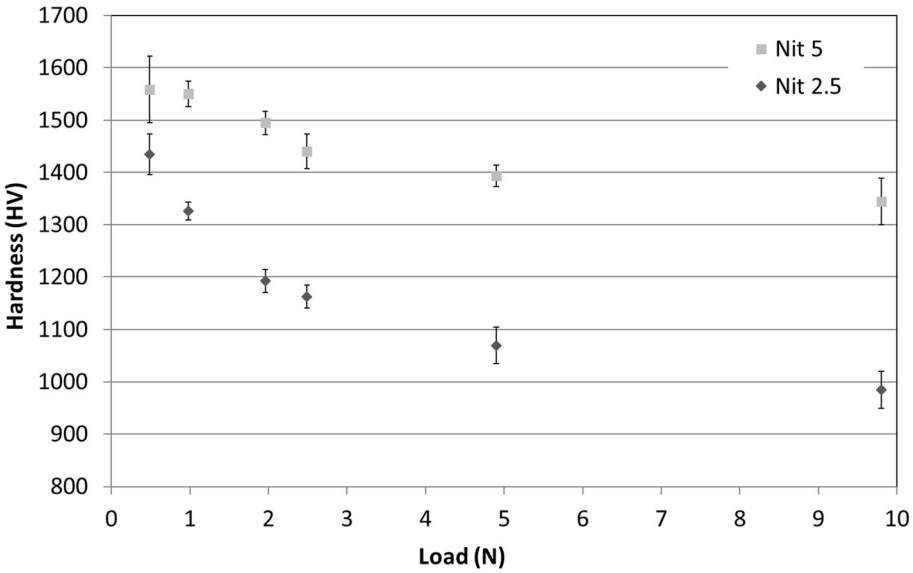

Fig. 5 Surface hardness of nitrided samples measured with different loads

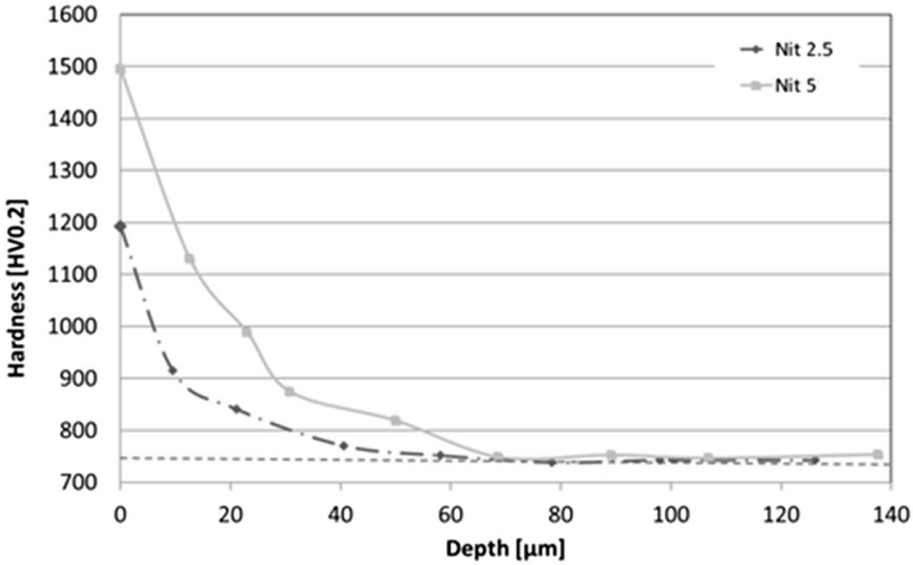

Fig. 6 Hardness as a function of depth for two nitrided samples

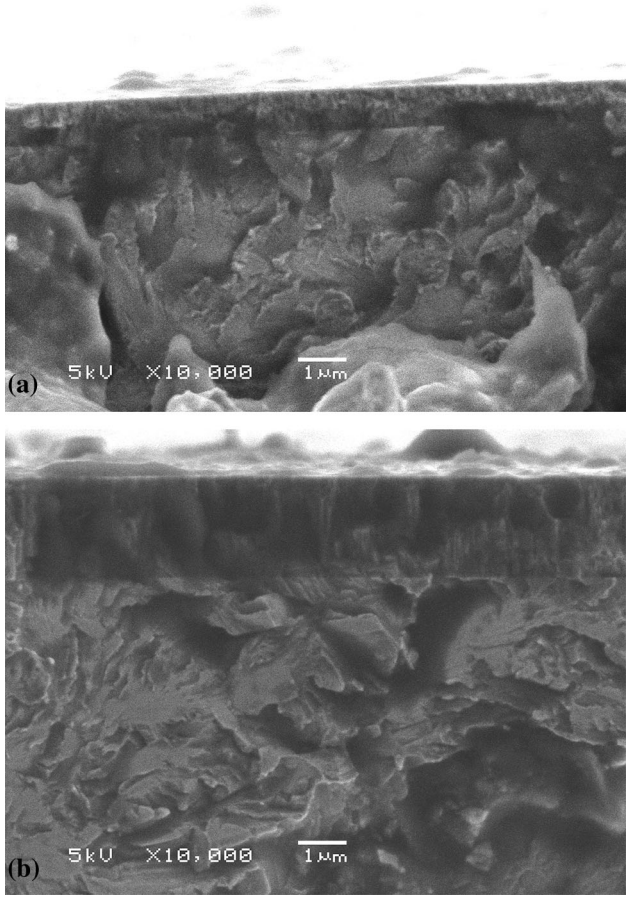

Fig. 7 Cross-section SEM images of coated samples (a) TiCN1 and (b) TiCN2

Table 4 presents the values of Young's modulus (E) as measured by nanoindentation. For all studied coating conditions, E decreases with nanoindentation load. However, for the samples with the duplex treatment (nitrided + coating), it is possible to observe that the reduction of E with load is lower

Table 4 Young's modulus values for different nanoindentation loads for all fabricated samples

Nanoindentation load Samples	Young's modulus, GPa		
	25, mN	50, mN	100, mN
Non-nitrided	273.0 ± 11	254.6 ± 3	240.9 ± 10
Nit 2.5	303.2 ± 10	273.2 ± 7	257.9 ± 4
Nit 5	285.0 ± 5	272.5 ± 6	256.4 ± 5
TiCN1	473.5 ± 26	302.1 ± 12	243.3 ± 5
TiCN2	553.3 ± 27	422.8 ± 10	299.1 ± 15
Nit 2.5 + TiCN1	429.6 ± 23	331.1 ± 8	276.2 ± 12
Nit 2.5 + TiCN2	548.2 ± 28	427.2 ± 10	344.3 ± 27
Nit 5 + TiCN1	428.2 ± 11	357.1 ± 11	298.2 ± 11
Nit 5 + TiCN2	546.6 ± 10	444.7 ± 15	358.2 ± 8

(especially for the 5-h nitriding treatment). Apart from the case of 25 mN load, the maximum indentation depth exceeded 10% of the coating thickness, resulting in the substrate influencing the measurements. This reduction in E is consistent with the observed reduction in hardness.

Figure 8(a) shows the XRD peaks for nitrided and non-nitrided samples. The nitrided conditions are Nit 2.5 and Nit 5.0, for nitriding times of 2.5 and 5.0 h, respectively. A displacement of α-Fe peaks for nitrided samples to the left in relation to the standard diffractogram position (e.g., for a non-nitrided sample) is a result of compressive residual stresses. The peak for the γ' -Fe_4N is seen for both Nit 2.5 and Nit 5.0 conditions, but in the metallographic analysis, no continuous white layer could be detected. The presence of this nitride cannot be neglected, as it can result from conical precipitations on the surface and being affected by preferred orientation (what would explain why the other peaks from this nitride are not seen), but the continuous layer is not formed. The absence of a significant number of other nitride peaks in the diffractograms with significant intensity and quantity, combined with the metallographic analysis, ensures that there was no continuous white layer formed in the surface of the nitrided samples for both treatment times.

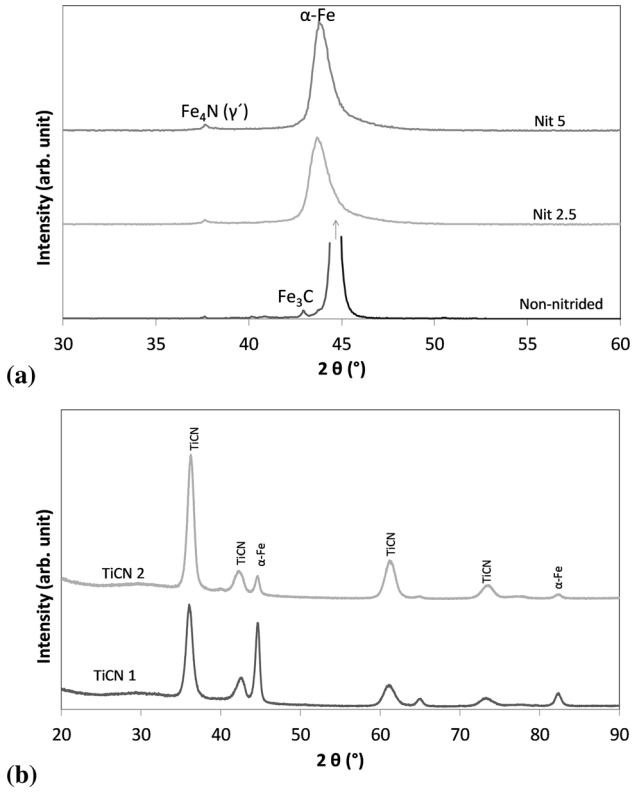

Fig. 8 X-ray diffractograms for phase analysis from (a) nitrided and non-nitrided samples and (b) TiCN1 and TiCN2 samples

Figure 8(b) presents the diffractograms for the coated samples. The main diffraction peaks identified belong to the TiCN compound for the treatment conditions TiCN1 and TiCN2. The peaks for α-Fe also appear due to the radiation penetration depth, which increases with decreasing 2θ, as the measurements kept the Bragg-Brentano condition. As the coating thickness increases from TiCN1 to TiCN2, the α-iron peak intensity decreases, and the TiCN peak intensity increases.

4.3 Nanohardness as a Function of Load

Figure 9, 10, and 11 shows the nanohardness values measured using loads of 25, 50, and 100 mN, respectively. In the case of non-nitrided samples, the hardness generally decreased with increasing measurement load. In the case of the 25 mN load (Fig. 9), the thicker coating (TiCN2) showed higher hardness values than the thinner one (TiCN1). Also, no influence of the nitriding layer was seen in the coating nanohardness at 25 mN load.

Figure 10 shows the results of nanohardness for the indentation load of 50 mN. As the penetration depth increased compared to 25 mN, higher hardness values of the coatings deposited on the previously nitrided substrate (duplex treatment) were observed for the samples with TiCN1 coatings. Yet, for the 2.5 h + TiCN1 duplex treatment, the hardness increased compared to the samples that were just nitrided for 2.5 h or just coated with TiCN1. For the 5 h + TiCN1 duplex treatment, the effect of the nitrided case in the hardness is even higher. For TiCN2-coated samples, the increase in the measuring load from 25 mN (Fig. 9) to 50 mN (Fig. 10) did not change the nanohardness values due to the coating thickness; at this thickness (TiCN2), the coating supports most of the load.

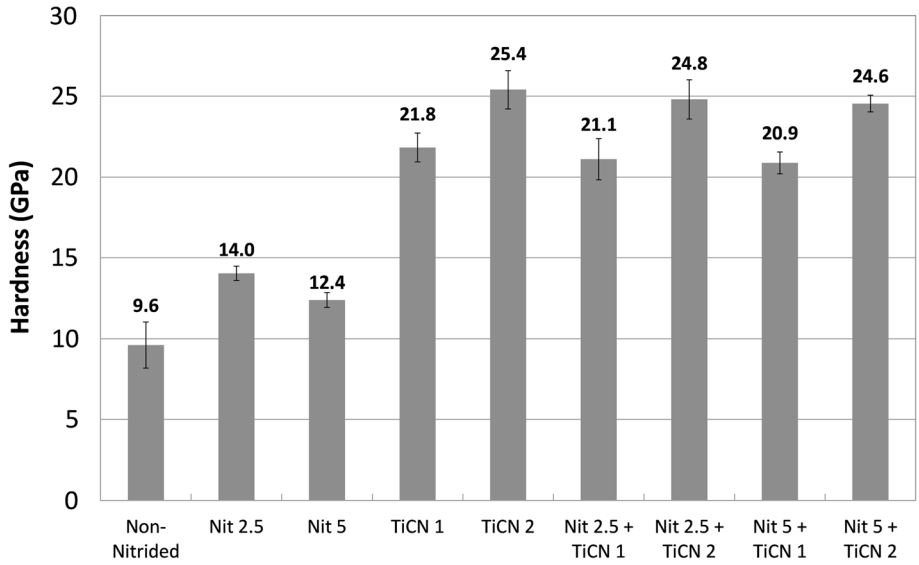

Fig. 9 Nanohardness values obtained with a 25-mN load

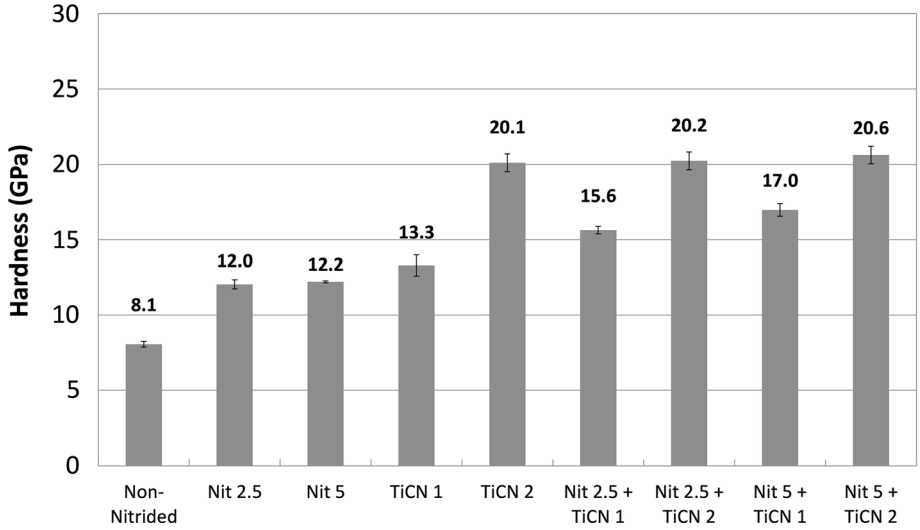

Fig. 10 Nanohardness values obtained with a 50-mN load

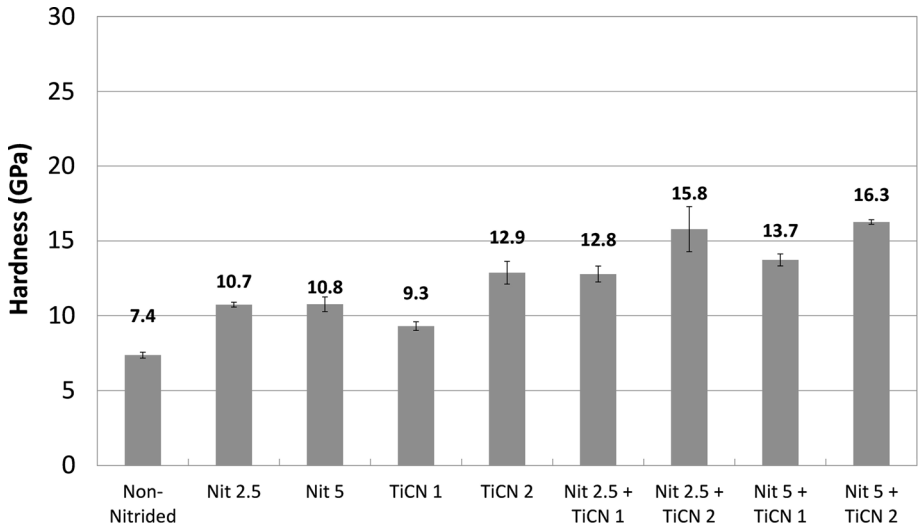

Fig. 11 Nanohardness values obtained with a 100-mN load

The results for the hardness at 100 mN are presented in Fig. 11. The hardness of the samples coated with TiCN1 increased, from 9.3 GPa, for just coated samples, to 12.8 GPa and 13.7 GPa, for the TiCN1 on nitrided substrates during 2.5 and 5 h, respectively. The same trend was observed for samples coated with TiCN2. The TiCN2 hardness remained 12.9 GPa for just coated samples, while duplex treated samples showed hardness of 15.8 and 16.3 GPa for TiCN2 over nitriding cases obtained with 2.5 and 5 h, respectively. Therefore, the higher hardness values for duplex treated samples shown in Fig. 10 and 11 for the higher loads and, consequently higher penetration depths, are a consequence of an increase in the load-bearing capacity given by the plasma-nitrided case.

4.4 Influence of Carbon Content on the Coating Hardness

Figure 12 shows the relative carbon atomic fraction profiles C/(C+N) for the TiCN thin films as a function of depth. The carbon atomic fraction in TiCN1 from the coating surface (0 μm) to approximately 0.25 μm oscillated around 0.5 C/(C+N). The fraction decreases linearly to a minimum at the opposite side of the coating layer (the interface between the coating and substrate), resulting in a value of approximately 0.075 C/(C+N).

In the case of the TiCN2 thin film, three distinct regions were observed in the carbon atomic fraction profile. The first region, from the coating surface to a thickness of ~0.25 μm, showed a carbon atomic fraction decaying from 0.5 to 0.3. In the second region, from about 0.25 to 1.1 μm, the carbon atomic fraction stayed constant, with a value of about 0.22. In the third region, from 1.1 to 2.0 μm (near the interface of the coating layer with the substrate), a new linear relationship was established, where C/(C+N) decreased down to 0.1 in the coating/substrate interface.

Yasuoka et al. (Ref 23) studied single TiCN coatings by varying the atomic fraction of carbon in the films. They concluded that increasing the atomic fraction of carbon in the film resulted in the substitution of N by C in the TiCN structure that increased crystal lattice stresses in the coating, which in turn increased the hardness. The film with the highest hardness had a carbon fraction of 0.5.

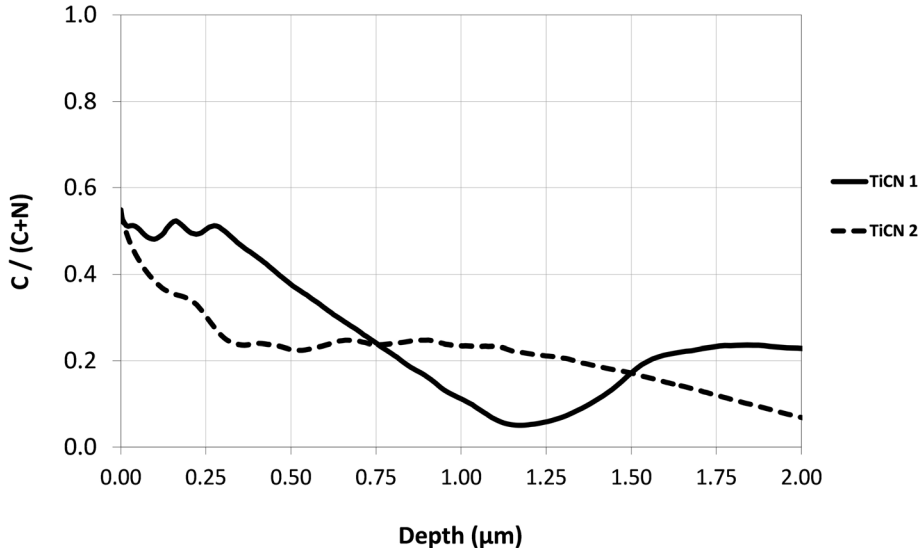

Fig. 12 Carbon atomic fraction profile for the TiCN1 and TiCN2 coatings

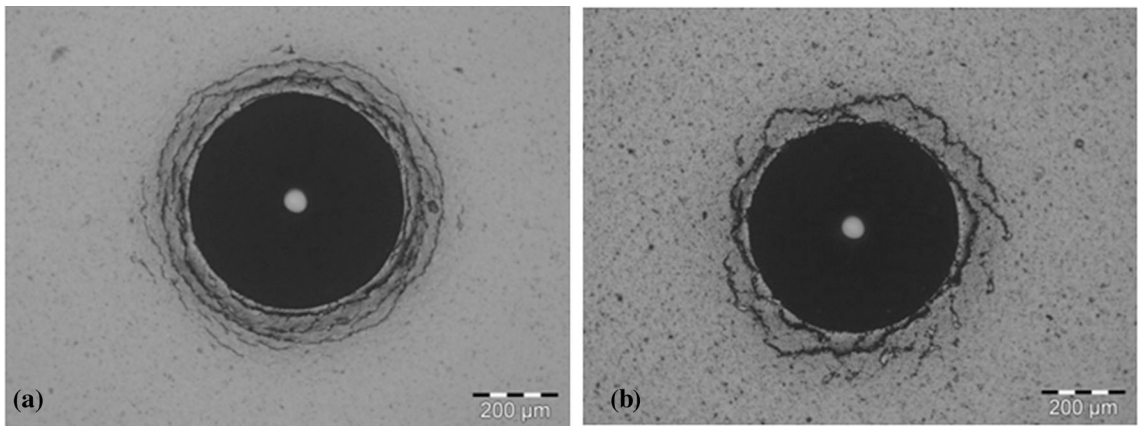

Fig. 13 Indentation patterns for the (a) TiCN1 sample (HF5: bad adhesion) and (b) TiCN2 sample (HF6: bad adhesion)

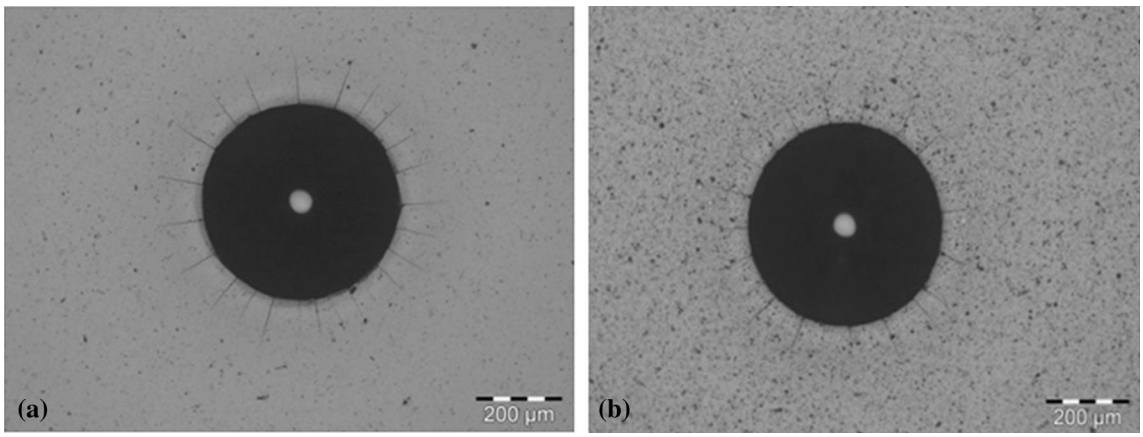

Fig. 14 Indentation patterns for the (a) Nit 2.5 + TiCN1 sample (HF1: good adhesion) and (b) Nit 2.5 + TiCN2 sample (HF1: good adhesion)

The TiCN1 film had a higher carbon fraction throughout the entire coating thickness compared to TiCN2, but presented lower measured nanohardness values, which can only be understood by its lower thickness, half of the TiCN2.

4.5 Coating Adhesion

The results for the indentation tests carried out on TiCN1 and TCN2 coatings over non-nitrided substrates are shown in

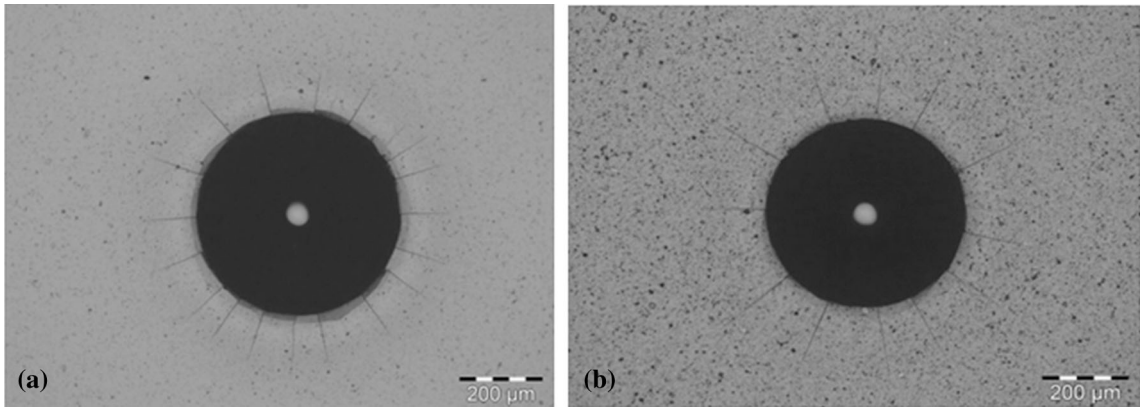

Fig. 15 Indentation patterns for the (a) Nit 5 + TiCN1 sample (HF1: good adhesion) and (b) Nit 5 + TiCN2 sample (HF1: good adhesion)

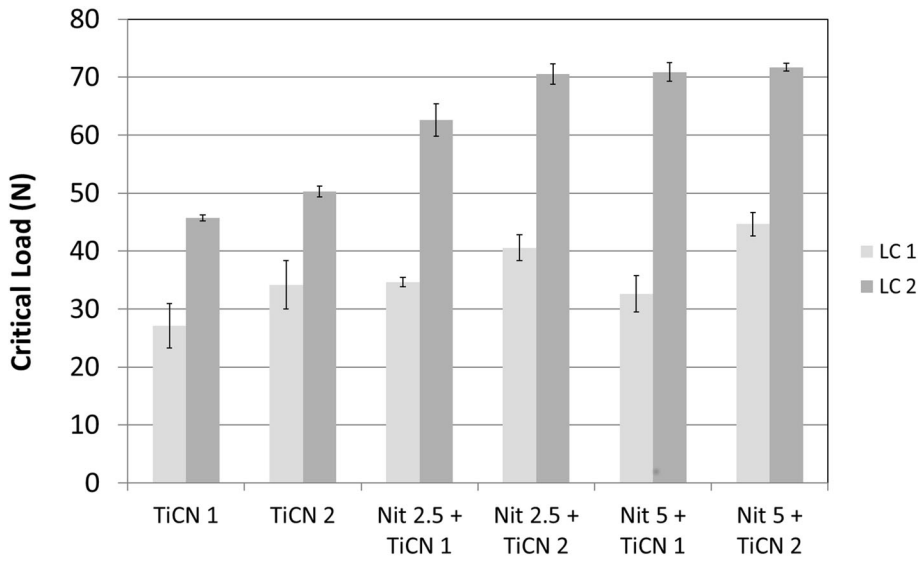

Fig. 16 Critical loads Lc1 and Lc2 for the different samples produced

Fig. 13. Peripheral cracks were observed around the indentation for both coatings (13a and 13b), where the surrounding areas of the coating already showed some delaminated regions. This type of failure pattern indicates a lack of load bearing capacity and poor adhesion. In this case, although the visual pattern of indentation did not fit those presented in the DIN 4856 standard, the adhesion was considered unsatisfactory. Also, Fig. 13(a) shows a lower exposure of the substrate in the case of the TiCN1 coating (thin) compared to the TiCN2 (thick) presented in Fig. 13(b). This indicates a better adhesion of the thinner coating in this test.

Figures 14 and 15 shows the adhesion results for TiCN1 and TiCN2 over nitrided substrates. The cracks features indicate excellent adhesion of the coating; significantly fewer cracks were observed for the samples previously nitrided during 5 h (Fig. 15) compared with the 2.5 h (Fig. 14). Compared to the DIN 4856 standard, all images presented in Fig. 14 and 15 were considered to show good adhesion as the films remained well adhered to the nitrided substrates.

Although scratch test results are a combination of deformation, adhesion, and internal stresses, it is a well-accepted testing method for qualitative evaluation of adhesion. The scratch tests result for all samples is shown in Fig. 16. For the non-nitrided substrates, Lc1 was higher for TiCN2 than TiCN1. The value of Lc2 was also measured, which indicates the adhesion strength at the coating–substrate interface. The TiCN2 coating showed a better ability to remain adhered to the substrate and support failures, reaching an average Lc2 of 50.3 N, while TiCN1 provided a lower average Lc2 value of 45.7 N. Also, this figure shows that, in general, the two different plasma nitriding conditions applied before coating were able to increase both

Table 5 Scratch crack propagation resistance (CPRs) values

Samples	CPRs
TiCN1	504
TiCN2	550
Nit 2.5 + TiCN1	883
Nit 2.5 + TiCN2	1216
Nit 5 + TiCN1	1246
Nit 5 + TiCN2	1207

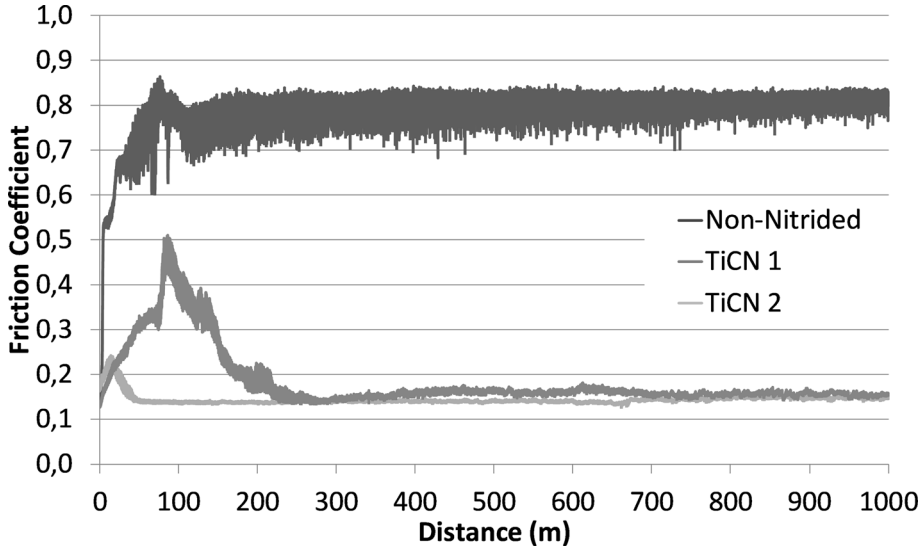

Fig. 17 Ball-on-disc friction coefficient for non-nitrided vs. TiCN1 and TiCN2 samples

Lc1 and Lc2 compared to the values achieved without nitriding. In the case of TiCN2, Lc2 was significantly higher for the nitrided substrate. However, the nitriding time did not significantly affect the critical load improvement, with a 40% improvement for 2.5-h nitriding time (Nit 2.5 + TiCN2) and 43% for the 5.0-h nitriding time for the Nit 5 + TiCN2 condition.

The thicker coatings (TiCN2) showed slightly higher Lc1 values than the thinner films (TiCN1). Analyzing the influence of the coating thickness on the critical loads, Cassar et al. (Ref 24) observed no consensus on this point; increased critical loads have been measured for thicker coatings, while they also generally have higher residual stresses, degrading adhesion and enhancing delamination. Experimental studies by Rickerby et al. (Ref 25) and Lin et al. (Ref 26) showed that a reduction in the critical loads is expected when the residual stresses in TiN coatings deposited by PVD increases. This is a result of the stored internal energy and interface stresses increasing the likelihood of adhesion failures. These authors also reported that the critical load varies inversely with compressive residual stresses. The total stress is the result of the superimposition of the stresses caused by the movement of the indenter and the compressive residual stresses in the coating. Thus, high residual stresses in a coating reduce the energy required to remove it from the substrate (adhesive failure) during the scratch test.

An important factor is how the coating supports the propagation of cracks up to the point of delamination, which serves as a criterion for determining the quality of a duplex system (Ref 27). According to Li et al. (Ref 28), the relationship that correlates Lc1 and Lc2 is the scratch crack propagation resistance (CPRs), as shown by the equation: CPRs = Lc1*(Lc2-Lc1), where the CPRs values indicate the toughness of the coating system.

Table 5 shows the CPRs values for the tested samples. The coatings applied over nitrided substrates supported the propagation of cracks without delamination, indicating that the higher CPRs values correspond to better adhesion. These values show the benefits of coatings that remain well adhered to previously nitrided substrates in comparison with non-nitrided ones. The nitrided layer imparts several benefits, including an increase in surface yield strength (a higher critical load is required for coating failure) and enhanced adhesion due to interdiffusion at the interface by the high affinity between N and Ti (the first layer deposited before the formation of the TiCN in the coating process). As reported by Baek et al. (Ref 13), the interdiffusion that takes place during the deposition process results in the formation of additional TiN, which improves adhesion. Finally, the resistance to crack propagation of the coating itself is important, which was higher for TiCN2 coating than the TiCN1 coating (considering the CPRs values obtained on non-nitrided substrates). Therefore, both the coating and substrate clearly contributed to the improved adhesion.

The ball-on-disc tribological test results for only coated samples, conditions TiCN1 and TiCN2 (without duplex treatment) and for a non-nitrided sample as reference are presented in Fig. 17. There is a significantly reduction of friction coefficient with the use of the coatings. However, a significant longer distance is related to the running-in effect for the TiCN2 condition compared to the TiCN1 condition. The distance for running-in for the TiCN1 sample was 50 m, whereas in the TiCN2 sample was 250 m. After running-in, both coatings present similar friction coefficients, around 0.15 against 0.8 for non-coated ones. The friction coefficient peaked is 0.50 for TiCN2 and 0.24 for TiCN1 in the running-in period of the tribological tests

Figure 18a presents the TiCN1 friction coefficient behavior on nitrided and non-nitrided substrates. For this thinner coating condition, the combination of nitriding with the coating did not change the friction coefficient significantly after running-in compared to just coated samples. However, nitriding influenced the running-in regime; as the nitriding time increases, the running-in distance also increases. This behavior can be explained by the higher load-bearing capacity, which decreased the wear rate during running-in. In the case of coating TiCN2 (Fig. 18b), as coating thickness increases, the effect of increasing running-in distance is not pronounced. Additionally, coating condition TiCN2, independently from the previous nitriding, presented slightly higher friction coefficients than TiCN1, which can be related to the different coating parameters set to achieve a thicker layer in TiCN2.

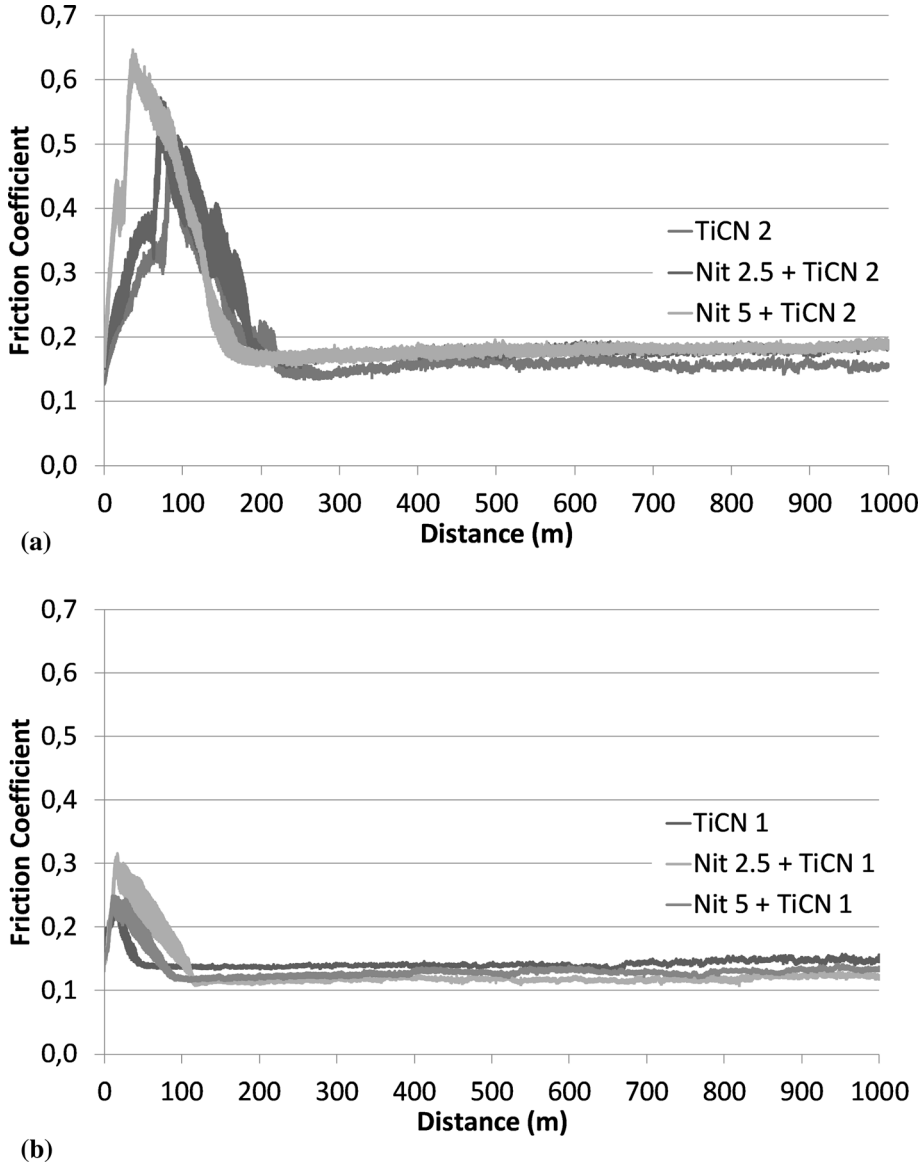

Fig. 18 Ball-on-disc friction coefficient for the different coating systems (a) TiCN1, TiCN1 + 2.5 h and TiCN1 + 5.0 h and (b) TiCN2, TiCN2 + 2.5 h and TiCN1 + 5.0 h

Figure 19 presents the SEM images of the surface before the samples have been submitted to the ball on disc tests (Fig. 19a and b) and the resulting wear tracks after the tests (Fig. 19c and d). The TiCN2 coating presented a higher quantity of pores and in a larger number compared to the TiCN1 surface. This was probably due to the high deposition rate used to obtain the coating TiCN2 than TiCN1, 3.0 μm/h, and 1.9 μm/h, respectively. The TiCN1 lower friction coefficient is and shorter running-in, observed in Fig. 18, is associated with the lower porosity. These clear differences observed between these test results for both coatings can be also verified through an analysis of the wear tracks on the samples nitrided for 2.5 h and coated, presented in Fig. 19(c) for TiCN1 and 19(d) for TiCN2. The track created in the TiCN2 is wider and deeper than TiCN1, indicating more severe wear in the TiCN2. Similar behavior was verified for the tracks with other tested conditions.

4.6 General Aspects

Table 6 presents a summary of the main results. Both tested coatings produced a poor adhesion in non-nitrided substrates, as seen from the adhesion DIN 4856 tests. When duplex treatment was applied, the scratch tests revealed that adhesion problem was solved. The nitriding treatments improved load-bearing capacity, according to the nanohardness results. When comparing the nitriding treatments, it is possible to observe that 5.0-h treatment resulted in higher surface hardness and a deeper diffusion zone than the 2.5-h treatment.

The combination of TiCN1, due to its lower thickness, with the thinner diffusion layer produced by 2.5 h nitriding (condition Nit 2.5 + TiCN1), presented a lower critical load in the scratch test. Therefore, the three last conditions in Table 6 can be considered as the best choices for application. The performance of Nit 5 + TiCN1 in the scratch test (CPRs 1246) was slightly

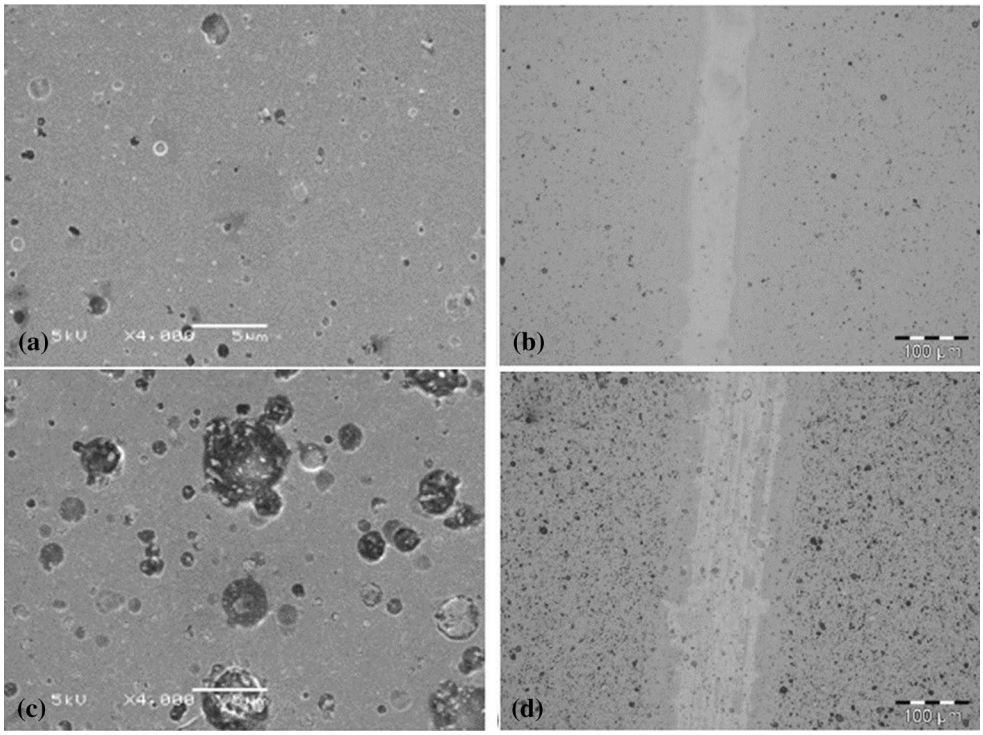

Fig. 19 SEM images of the surface before ball-on-disc tests for (a) TiCN1 and (b) TiCN2. Resulting ball-on-disc tracks for (c) TiCN1 + 2.5 h and (d) TiCN2 + 2.5 h

Table 6 Summary of test results

	Nanohardness (GPa) [*Young's module (E)*]					
Samples	**25, mN**	**50, mN**	**100, mN**	**Adhesion DIN 4856**	**CPRs**	**Friction coefficient (peak)**
TiCN1	21.8 [*473*]	13.3 [*302*]	9.3 [*243*]	Poor	504	0.15 (0.24)
TiCN2	25.4 [*553*]	20.1 [*422*]	12.9 [*299*]	Poor	550	0.16 (0.50)
Nit 2.5 + TiCN1	21.1 [*429*]	15.6 [*331*]	12.8 [*276*]	Good	883	0.14 (0.26)
Nit 2.5 + TiCN2	24.8 [*548*]	20.2 [*427*]	15.8 [*344*]	Good	1216	0.18 (0.58)
Nit 5 + TiCN1	20.9 [*428*]	17.0 [*357*]	13.7 [*298*]	Good	1246	0.13 (0.32)
Nit 5 + TiCN2	24.6 [*546*]	20.6 [*444*]	16.3 [*358*]	Good	1207	0.18 (0.64)

better than the other two duplex treatments with TiCN2. The surface nanohardness with 50mN load gave values above 20 GPa for the combinations with TiCN2 coating while the Nit 5+TiCN1, the hardness was 17 GPa. However, 17 GPa is already a significantly high value for most applications; it is two times higher than the substrate hardness. The friction coefficient values for the Nit 5 + TiCN1 combination is 0.13, while both TiCN2 combinations are 0.18. This lower friction coefficient of TiCN1 is also evident in the analysis of ball-on-disc wear tracks.

Therefore, in this work the overall best properties were presented by the duplex treatment conditions Nit 5 + TiCN1, being the combination of a thinner TiCN coating with a deeper plasma nitriding diffusion layer.

5. Conclusions

In this work, a DIN X100CrMoV8-1-1 cold work tool steel was plasma nitrided, using a 5 vol-%. N_2 + 95 vol-% H_2 gas mixture, for 2.5- or 5.0-h nitriding times, generating different substrates. The substrates were coated with TiCN by PVD cathodic arc evaporation to generate coating thicknesses of about 1 and 2 μm on each substrate (identified as coating variants TiCN1 and TiCN2). Hardness, adhesion, and friction tests were carried out to characterize the different combinations. The main conclusions are given as follows:

- Plasma nitriding with 5 vol-%. N_2 + 95 vol-% H_2 gas mixture avoided compound layer formation, giving a diffusion zone with a surface hardness 50% higher than core and depths of 58 μm and 68 μm for 2.5-h and 5.0-h nitriding times, respectively.
- One of the TiCN coating investigated in this work, identified as TiCN1, presented a higher carbon atomic fraction compared to the second coating, TiCN2. However, due to the lower thickness of TiCN1, this higher carbon atomic fraction did not reflect a higher measured hardness.
- TiCN coatings significantly reduced the friction coefficients in the ball-on-disc tests, from values of 0.8 for non-nitrided samples (without coating) to values of 0.14-0.18 for coated ones (for non-nitrided and nitride substrates).

However, the thicker TiCN coating (TiCN2) presented higher friction coefficients (about 0.18) and wider wear tracks when compared to the thinner coatings (about 0.14). The increase in the deposition rate to obtain a thicker coating led to a coating with higher amount of porosity (TiCN2), which was the main influence on the friction coefficient and wear results.

- Unsatisfactory adhesion revealed by coating delamination in the TiCN coating deposited on non-nitrided substrates, regardless of the coating thickness. This clearly showed a lack of substrate mechanical support and adhesion. Plasma nitriding with no compound layer proved to be a good microstructure to improve adhesion of both TiCN coating thicknesses (with 1 and 2 μm thickness), as it changed the result of the DIN 4856 test from poor to good and high scratch crack propagation resistance from values of about 525 to 1225. The best results were achieved with deeper plasma nitriding diffusion zones (resulted from 5-h nitriding time), due to its high load-bearing capacity, leading to higher measured hardness and scratch crack propagation resistance.

Acknowledgements

The authors would like to thank CNPq (the Brazilian National Council for Scientific and Technological Development) for the financial support under the framework of the PQ scholarship process, Grant Numbers 311348/2015-7, 149850/2010-7, and 162290/2014-4.

References

1. Y.-Y. Chang and S. Amrutwar, Effect of Plasma Nitriding Pretreatment on the Mechanical Properties of AlCrSiN-coated Tool Steels, *Materials*, 2019, **12**(5), p 795
2. A.F. Rousseau et al., Microstructural and Tribological Characterisation of a Nitriding/TiAlN PVD Coating Duplex Treatment Applied to M2 High Speed Steel Tools, *Surf. Coat. Technol.*, 2015, **272**, p 403–408
3. B. Podgornik, J. Vizintin and V. Leskovsek, Wear Properties of Induction Hardened, Conventional Plasma Nitrided and Pulse Plasma Nitrided AISI 4140 Steel in Dry Sliding Conditions, *Wear*, 1999, **232**, p 231–242
4. C. Mendibide, P. Steyer, J. Fontaine and P. Goudeau, Improvement of the Tribological Behaviour of PVD Nanostratified TiN/CrN Coatings - An Explanation, *Surf. Coat. Technol.*, 2006, **201**, p 4119–4124
5. F. Klocke and H.-W. Raedt, Formulation and Testing of Optimised Coating Properties with Regard to Tribological Performance in Cold Forging and Fine Blanking Applications, *Int. J. Refract. Met. Hard Mater.*, 2001, **19**, p 495–505
6. L. Llanes, E. Tarrés, G. Ramírez, C. Botero and E. Jiménez-Piqué, Fatigue Susceptibility Under Contact Loading of Hardmetals Coated with Ceramic Films, *Procedia Eng.*, 2010, **2**, p 299–308
7. W. Zhao and D. Kong, Microstructure, Bonding Strength, and Friction–Wear Performance of AlCrN/nitrided Layer Composite Coating on H13 Hot Work Mould Steel, *Int. J. Appl. Ceram. Technol.*, 2019, **16**(3), p 951–965
8. Y. Deng et al., Effects of Tailored Nitriding Layers on Comprehensive Properties of Duplex Plasma-treated AlTiN Coatings, *Ceram. Int.*, 2017, **43**(12), p 8721–8729
9. G.B. Both, A.S. Rocha, G.R. Santos and T.K. Hirsch, An Investigation on the Suitability of Different Surface Treatments Applied to a DIN X100CrMoV8-1-1 for Cold Forming Applications, *Surf. Coat. Technol.*, 2014, **244**, p 142–150
10. V. Podgurskya, R. Nisumaa, E. Adoberg, A. Surzhenkov, A. Sivitski and P. Kulu, Comparative Study of Surface Roughness and Tribological Behavior During Running-in Period of Hard Coatings Deposited by Lateral Rotating Cathode Arc, *Wear*, 2010, **268**, p 751–755
11. K. Holmberg, A. Matthews and H. Ronkainen, Coatings Tribology - Contact Mechanisms and Surface Design, *Tribol. Int.*, 1998, **31**, p 107–120
12. S. Baragetti and F. Tordini, Fatigue Resistance of PECVD Coated Steel Alloy, *Int. J. Fatigue*, 2007, **29**, p 1832–1838
13. W.-S. Baek, S.-C. Kwon, S.-R. Lee, J.-J. Rha, K.-S. Nam and J.-Y. Lee, A Study of the Interfacial Structure Between the TiN Film and the Iron Nitrided Layer in a Duplex Plasma Surface Treatment, *Surf. Coat. Technol.*, 1999, **144**, p 94–100
14. J.C.A. Batista et al., Process Developments Towards Producing Well Adherent Duplex PAPVD Coatings, *Surf. Eng.*, 2003, **19**(1), p 37–44
15. S.C. Lee, W.Y. Ho and W.L. Pao, Process and Properties of CrN Coating Deposited on Plasma Nitrided High-speed Steel, *Surf. Coat. Technol.*, 1995, **73**(1–2), p 34–38
16. J. Zheng et al., Microstructures and Mechanical Properties of Duplex-treated Composite Ceramic Coatings with and Without Compound Layer, *Ceram. Int.*, 2015, **41**(2), p 2519–2526
17. W. Chen et al., Comparison of AlCrN and AlCrTiSiN Coatings Deposited on the Surface of Plasma Nitrocarburized High Carbon Steels, *Appl. Surf. Sci.*, 2015, **332**, p 525–532
18. C. Kwietniewski and A. da Silva Rocha, Nitrided Layer Embrittlement due to Edge Effect on Duplex Treated AISI M2 High-speed Steel, *Surf. Coat. Technol.*, 2004, **179**, p 27–32
19. S. Rocha, T.R. Strohaecker, V. Tomala and T.K. Hirsch, Microstructure and Residual Stresses of a Plasma-nitrided Tool Steel, *Surf. Coat. Technol.*, 1999, **115**, p 24–31
20. A. Rocha and T. Hirsch, Effect of Different Surface States Before Plasma Nitriding on Properties and Machining Behavior of M2 High-speed Steel, *Surf. Coat. Technol.*, 2003, **165**, p 176–185
21. Carbon-based films and other hard coatings - Rockwell penetration test to evaluate the adhesion, Standard number: DIN 4856, Deutsches Institut für Normung e.V., 2018-02
22. M. Müser and L. Valentin, Popov: Contact Mechanics and Friction: Physical Principles and Applications, *Tribol. Lett.*, 2010, **40**, p 395
23. M. Yasuoka, P. Wang and P. Murakami, Comparison of the Mechanical Performance of Cutting Tools Coated by Either a TiC_xN_{1-x} Single-layer or a $TiC/TiC_{0.5}N_{0.5}/TiN$ Multilayer Using the Hollow Cathode Discharge Ion Plating Method, *Surf. Coat. Technol.*, 2012, **206**, p 2168–2172
24. G. Cassar, S. Banfield, J.C. Avelar-Batista, J. Housden and A. Matthews, Tribological Properties of Duplex Plasma Oxidized, Nitrided and PVD Coated Ti–6Al–4V, *Surf. Coat. Technol.*, 2011, **206**, p 395–404
25. D.S. Rickerby and P.J. Burnett, The Relationship Between Hardness and Scratch Adhesion, *Thin Solid Films*, 1987, **154**, p 403–416
26. C.H. Lin, H.L. Wan and M.H. Hon, The Effect of Residual Stress on the Adhesion of PECVD- Coated Aluminum Oxide Film of on Glass, *Thin Solid Films*, 1996, **283**, p 171–174
27. S. Zhang, D. Sun, Y. Fu and H. Du, Effect of Sputtering Target Power on Microstructure and Mechanical Properties of Nanocomposite nc-TiN/a-SiN_x Thin Films, *Thin Solid Films*, 2004, **462**, p 447–448
28. S. Zhang and X. Zhang, Toughness Evaluation of Hard Coatings and Thin Films, *Thin Solid Films*, 2012, **520**, p 2375–2389